IMAGE DENOISING USING A TIGHT FRAME

L. Shen, M. Papadakis†, I.A. Kakadiaris‡, I. Konstantinidis‡, D. Kouri§, D. Hoffman¶*

ABSTRACT

We present a general mathematical theory for lifting frames that allows us to modify existing filters to construct new ones that form Parseval frames. We apply our theory to design non-separable Parseval frames from separable (tensor) products of a piecewise linear spline tight frame. These new frame systems incorporate the weighted average operator and the Sobel operator in directions that are integer multiples of 45^o. A new image denoising algorithm is then proposed tailored to the specific properties of these new frame filters. We demonstrate the performance of our algorithm on a diverse set of images with very encouraging results.

1. INTRODUCTION

Digital images are often degraded by noise in the acquisition and/or transmission phase. The goal of image denoising is to recover the true/original image from such a distorted/noisy copy. This is accomplished via a combination of methods involving suitable filtering/transforms and statistical estimation. Typically, the image is transformed onto some domain where the noise component can be identified more easily, and a statistical estimation is performed to identify and remove its influence.

In recent years, a wide class of image denoising algorithms have been based on the discrete wavelet transform. The usefulness of the wavelet transform was first demonstrated by Donoho and Johnstone [1, 2, 3], when they proved that thresholding estimators in a wavelet basis have nearly minimax risk for sets of piecewise regular images. For the case of additive Gaussian noise they suggested two thresholding functions, the soft-threshold $\eta_T^S(x) = \mathrm{sgn}(x)\cdot\max(|x|-T, 0)$ and the hard-threshold $\eta_T^H(x) = (x \text{ or } 0)$, depending on whether $|x| > T$ or not, respectively. The threshold T is to be selected using VisuShrink [1] or SureShrink [3].

Coifman and Donoho [4] established that the use of undecimated transforms minimizes artifacts in the denoised data; their translation invariant denoising scheme is equivalent to thresholding in the shift-invariant redundant representation implemented by a non-subsampled filter bank, or frame. In addition, it has been shown [5, 6, 7, 8] that a redundant representation is substantially superior to a non-redundant representation for image denoising in terms of mean-squared error and signal-to-noise ratio.

Several different types of frames have been applied to image denoising, such as the “steerable pyramid” [9, 10] and the dual-tree complex wavelet transform [11, 12, 13]. To improve the selection criteria for the threshold T, such methods depart from the minimax framework, which is optimal when no *a priori* information about the signal itself is assumed, and move to a Bayesian approach, where both the noise and the true image signal coefficients in the wavelet domain can be modeled using some prior distribution [14, 15, 6]. Even better results can be obtained by exploiting the fact that wavelet coefficients are statistically dependent [16, 17]. Recent examples include the bivariate model of Sendur and Selesnick [12, 13] and the Gaussian Scale Mixtures (GSM) model of Portilla *et al.* [10].

Our work in this paper complements the existing literature. We design non-separable Parseval frames from separable (tensor) products of a piecewise linear spline tight frame. These new non-separable frame systems incorporate the weighted average operator and the Sobel operator in directions that are integer multiples of 45^o. We propose a mixed thresholding strategy that is tailored to the specific operators in this tight frame and takes advantage of the dependencies between them.

The remainder of this paper is organized as follows. Section 2 provides a method of modifying existing frames in order to produce new ones and an application to construct a frame-based filtering scheme. This scheme is employed in Section 3 to design a denoising algorithm. Our experimental results are presented in Section 4, while our conclusions are given in Section 5.

2. CONSTRUCTING NEW FRAMELET FILTERS

As explained in the introduction, redundant representations, such as frames, are preferable for denoising purposes. Designing frames also proves to be more efficient than designing bases, especially when one designs Riesz or orthonormal bases in multi-dimensions arising from scaling functions [18]. A *Parseval frame* (PF) for a Hilbert space is a tight frame with bounds equal to 1. The advantage of PF versus other types of frames is that the same set of vectors can be used for decomposition and reconstruction, just as in the case of orthonormal bases. Exact frames (frames having no redundancy) are Riesz bases and vice-versa.

We define the translation operator $T_{\mathbf{n}}$ acting on $\ell^2(\mathbb{Z}^d)$ by $T_{\mathbf{n}}s(\mathbf{m}) = s(\mathbf{m}-\mathbf{n})$, for every $\mathbf{n}, \mathbf{m} \in \mathbb{Z}^d$. Our goal is to construct digital filters using the integer translates of certain finite-length filters. More precisely, the Hilbert space of digital signals we wish to work with in our applications is $\ell^2(\mathbb{Z}^d)$, where $d = 2$, although the results presented in this section hold true for any natural number d. An element K of $\ell^2(\mathbb{Z}^d)$ is a *digital filter* if its Fourier transform $\widehat{K}$ is a bounded function. This filter acts on every digital signal by convolution (i.e., $s \to s * K$, where $s \in \ell^2(\mathbb{Z}^d)$).

We begin by stating the following general result, the proof of which is based on Lemma 2.5 [19].

Proposition 1 *Assume that K_i, with $i = 0, 1, \ldots, l$ is a family of digital filters whose integer translates form a frame for $\ell^2(\mathbb{Z}^d)$. For a given positive integer p, let U be a $2\pi\mathbb{Z}^d$-periodic $(p+1)\times(l+1)$ matrix-valued function whose entries $(U(\omega))_{q,r}$ are continuous. If there exists $A > 0$ such that for almost every $\omega \in [-\pi,\pi)^d$ we have $A\|\mathbf{x}\| \le \|U(\omega)\mathbf{x}\|$ for all $\mathbf{x} \in \mathbb{C}^{l+1}$, then the*

*Dept. of Mathematics, Western Michigan U., Kalamazoo, MI 49008.
†Dept. of Mathematics, U. of Houston, Houston, TX 77204.
‡Visual Computing Lab, Dept. of Computer Science, U. of Houston, Houston, TX 77204.
§Depts. of Chemistry and Physics, U. of Houston, Houston, TX 77204.
¶Dept. of Chemistry and Ames Laboratory, Iowa State U., Ames, IA 50011.

matrix multiplication $U(\omega)(\widehat{K_0}(\omega), \widehat{K_1}(\omega), \ldots, \widehat{K_l}(\omega))^t$*, defines a new family of digital filters whose integer translates form a frame for* $\ell^2(\mathbb{Z}^d)$*. If, in particular,* $U(\omega)$ *is an isometry, for almost every* $\omega \in [-\pi, \pi)^d$*, then the resulting and the original frames have the same frame bounds.*

In particular, we use Prop. 1 to lift the frame described by Ron and Shen [20] as being the simplest example of a compactly supported tight spline frame. We select splines of degree one in order to keep the number of wavelets to a minimum. The low-pass m_0, bandpass m_1, and high-pass m_2 filters, associated with the scaling function ϕ and the two wavelets ψ_1 and ψ_2, respectively, are the following: $m_0(\omega) = \cos^2(\omega/2)$, $m_1(\omega) = i(\sqrt{2}/2)\sin(\omega)$, and $m_2(\omega) = \sin^2(\omega/2)$. Note that $|m_0(\omega)|^2 + |m_1(\omega)|^2 + |m_2(\omega)|^2 = 1$, for all $\omega \in [-\pi, \pi)$. Therefore, the translates $T_{\mathbf{n}}$ ($\mathbf{n} \in \mathbb{Z}$) of the impulse responses $h_0 = (1/4)\,[1, 2, 1]$, $h_1 = (1/4)\left[\sqrt{2}, 0, -\sqrt{2}\right]$ and $h_2 = (1/4)\,[-1, 2, -1]$ of m_0, m_1 and m_2 form a Parseval frame for $\ell^2(\mathbb{Z})$.

The Riesz scaling function ϕ and the wavelets ψ_1 corresponding to this frame have some interesting properties: 1) ϕ is interpolatory; 2) ϕ, ψ_1 and ψ_2 are supported on the interval $[-1, 1]$; and 3) ϕ and ψ_2 are symmetric while ψ_1 is anti-symmetric. Thus, ψ_1 can be used as a first-order singularity detector while ψ_2 can be used as a second-order singularity detector. This is the reason for selecting these framelets for the proposed denoising scheme.

The tensor product of this PF with itself forms nine separable (tensor product) filters: $m_{p,q}(\omega_1, \omega_2) = m_p(\omega_1)m_q(\omega_2)$, where $p, q \in \{0, 1, 2\}$. We have the following equality:

$$\sum_{p,q=0}^{2} |m_{p,q}(\omega)|^2 = 1, \quad \text{for} \quad \omega \in [-\pi, \pi)^2, \tag{1}$$

so this is another PF. We view $m_{0,0}$ as a low-pass filter, and the remaining eight filters as band-pass and high-pass. These filters comprise the UHF9 filter bank. Their corresponding filter taps are given by the nine 3×3 matrices $M_{p,q} := h_p^t h_q$.

We note that the filters $M_{0,1}$ and $M_{1,0}$ in the UHF9 filter bank are the Sobel operators detecting vertical and horizontal edges. This motivates us to augment bank UHF9 with two diagonal first order singularity detectors.

The UHF11 filter bank: Eq. (1) implies that vector v_1, given by: $v_1 := (m_{0,0}, m_{0,1}, m_{1,0}, m_{1,1}, m_{0,2}, m_{2,0}, m_{2,1}, m_{1,2}, m_{2,2})^t$ is unitary in $\mathbb{C}^9$ for every ω in $[-\pi, \pi)^2$. To construct the new filters, we first "clone" the pair of filters $(m_{0,1}, m_{1,0})$ into the quadruplet $(m_{0,1}, m_{1,0}, m_{0,1}, m_{1,0})$. To achieve this isometrically, we define the mapping $D := (1/\sqrt{2})[I_2 \quad I_2]^t$ from $\mathbb{C}^2$ into $\mathbb{C}^4$. We then use the rotation matrix $R := (1/\sqrt{2})[1 \quad 1; -1 \quad 1]$ to entwine the two new copies while leaving the originals unchanged. The result is the isometry matrix E:

$$E := \begin{bmatrix} I_2 & 0 \\ 0 & R \end{bmatrix} D = \begin{bmatrix} (1/\sqrt{2}) & 0 & (1/2) & -(1/2) \\ 0 & (1/\sqrt{2}) & (1/2) & (1/2) \end{bmatrix}^t.$$

Next, by considering the decompositions $\mathbb{C}^9 = \mathbb{C} \oplus \mathbb{C}^2 \oplus \mathbb{C}^6$ and $\mathbb{C}^{11} = \mathbb{C} \oplus \mathbb{C}^4 \oplus \mathbb{C}^6$, we define the matrix-valued function $U(\omega) := [1 \quad 0 \quad 0; 0 \quad E \quad 0; 0 \quad 0 \quad I_6]$, which is also unitary. Applying U to v_1 we derive another unit vector in $\mathbb{C}^{11}$ for every ω. By Prop. 1, $v_2 = Uv_1$ produces 11 filters whose integer translates generate a PF of $\ell^2(\mathbb{Z}^2)$. We call this the UHF11 filter bank. In summary, the UHF11 filter bank is implemented by the following filters: $K_0 = M_{0,0}$ is the low pass filter; the high–pass and band–pass filters are $K_1 = \frac{\sqrt{2}}{2}M_{0,1}$, $K_2 = \frac{\sqrt{2}}{2}M_{1,0}$, $K_3 = (1/2)(M_{0,1} + M_{1,0})$, $K_4 = (1/2)(M_{0,1} - M_{1,0})$, $K_5 = M_{1,1}$, $K_6 = M_{0,2}$, $K_7 = M_{2,0}$, $K_8 = M_{1,2}$, $K_9 = M_{2,1}$, and $K_{10} = M_{2,2}$.

We note that the second and third coordinates of v_2 still define the Sobel operators (scaled by $(1/\sqrt{2})$) in the horizontal and vertical directions, respectively. In addition, the impulse responses of the fourth and fifth coordinates of v_2 are given by:

$$\frac{\sqrt{2}}{8}\begin{bmatrix} 1 & 1 & 0 \\ 1 & 0 & -1 \\ 0 & -1 & -1 \end{bmatrix} \quad \text{and} \quad \frac{\sqrt{2}}{8}\begin{bmatrix} 0 & -1 & -1 \\ 1 & 0 & -1 \\ 1 & 1 & 0 \end{bmatrix},$$

respectively. These two filters act as derivatives parallel to the directions $(-\pi/4)$ and $(\pi/4)$ or, equivalently, as Sobel operators in these directions.

Several key properties of the Ron–Shen frame are also lifted to UHF9 and UHF11. The two frame wavelets ψ_1 and ψ_2 have vanishing moments of order 1 and 2, respectively (i.e., $\int \psi_1(x)\, dx = 0$ and $\int x^p \psi_2(x)\, dx = 0$ for $p = 0, 1$). Thus, constant signals cannot pass through the band–pass filter m_1, while neither constant nor linear signals can pass through the high–pass filter m_2. Due to the linearity of integration these properties impose similar characteristics to the UHF9 filter-bank which are subsequently inherited by the UHF11 filter bank.

The technique employed to construct the UHF11 filter bank relies on Prop. 1 in two ways. First, to construct isometries that increase the redundancy of an existing filter-based PF by producing scaled duplicates of certain of those filters; and second, to apply unitary operators on certain collections of those filters to produce new filters with desirable characteristics (e.g., geometry). In both cases the resulting frame is a Parseval frame. This is a versatile technique that can be employed in a much more general setting than the example discussed above.

3. PROPOSED ALGORITHMS

Let $\mathbf{X}$ be a noisy image. We filter $\mathbf{X}$ using the UHF11 filter bank. We stress that the outputs of this filter bank are undecimated. Let $\mathbf{Y}_m$ be the output of the image $\mathbf{X}$ through the m-th band (i.e., $\mathbf{Y}_m = \mathbf{X} * K_m$). We separate the ten high-pass subband outputs into two groups, $m = 1, \ldots, 5$ and $m = 6, \ldots, 10$, respectively. Note that filters in the first group can be used to detect first order singularities, while filters in the second group can be used to detect second order singularities. Accordingly, we choose different thresholding strategies for each of the two groups.

For the first group, we modify the coefficients in the $\mathbf{Y}_m$, $m = 1, \ldots, 5$ using the hard threshold operator η_T^H, where $T = \alpha \cdot \sigma_n \sqrt{2 \log N}$. Here α is a thresholding factor, N is the number of pixels in $\mathbf{X}$, and σ_n is the noise variance. The threshold $\sigma_n \sqrt{2 \log N}$ is a good choice for large values of N when a unitary wavelet transform is used [1]. However, the transforms induced by convolution with K_m are only isometric, and not unitary. This results in an overall reduction of the energy contribution of the noise in the transformed image [21]. Therefore, the threshold needs to be scaled by a factor α, where $0 < \alpha < 1$, which is selected experimentally. The criterion for its selection is the maximization of PSNR. If σ_n is not known, it is estimated by the robust median estimator $\widehat{\sigma} = \frac{1}{0.6745}\text{Median}(|\mathbf{Y}_{\text{Haar}}[i, j]|)$, where $\mathbf{Y}_{\text{Haar}}$ is the output of $\mathbf{X}$ using 1–level Haar high-pass filtering.

Our proposed algorithm jointly thresholds $\mathbf{Y}_1$ and $\mathbf{Y}_2$ to obtain $\widetilde{\mathbf{Y}}_1$, $\widetilde{\mathbf{Y}}_2$. It should be noted that the proposed shrinkage of the wavelet coefficients is not the same as the classical wavelet shrinkage. For $m = 1, 2$:

$$\widetilde{\mathbf{Y}}_m = \begin{cases} \mathbf{Y}_m, & \text{if } |\mathbf{Y}_m| > T_1 \text{ or } (|\mathbf{Y}_3| \text{ or } |\mathbf{Y}_4|) > T_2 \\ 0, & \text{otherwise} \end{cases} \quad (2)$$

where $T_1 = (1/2)T$ and $T_2 = (1/8)(2 + \sqrt{2})T$. These scaled thresholds are obtained by computing the maximum magnitude of the response of the filters K_1 and K_4, respectively. Similarly,

$$\widetilde{\mathbf{Y}}_m = \begin{cases} \mathbf{Y}_m, & \text{if } |\mathbf{Y}_m| > T_2 \text{ or } (|\mathbf{Y}_1| \text{ or } |\mathbf{Y}_2|) > T_1 \\ 0, & \text{otherwise} \end{cases} \quad (3)$$

for $m = 3, 4$. For $\mathbf{Y}_5$, we use the hard thresholding operator:

$$\widetilde{\mathbf{Y}}_5 = \eta^H_{T_1}(\mathbf{Y}_5). \quad (4)$$

Outputs in the second group are denoised by applying locally adaptive window-based denoising using MAP (LAWMAP) [15]. We assume that the coefficients $\mathbf{Y}_m[i,j]$ are independent zero-mean Gaussian variables with unknown variance $\sigma^2[i,j]$. An estimate of $\sigma^2[i,j]$ is formed based on a local neighborhood $\mathcal{N}_{i,j}$ which is a square window of size M centered at $\mathbf{Y}_m[i,j]$. We postulate an exponential prior $f_\sigma(\sigma^2) = \lambda\exp(-\lambda\sigma^2)$. Given this prior, the maximum a posteriori (MAP) estimator for $\sigma^2[i,j]$ is given by:

$$\tilde{\sigma}^2[i,j] = \frac{M}{4\lambda}\left[-1 + \sqrt{1 + (8\lambda/M^2)\sum \mathbf{Y}^2_m[p,q]}\right] - \sigma^2_n,$$

where the sum is over all $[p,q]$ in $\mathcal{N}_{i,j}$. We impose a positivity condition by setting all negative estimates equal to zero, as suggested by Mihcak *et al.* [15], since it is possible to obtain negative values from the actual MAP estimate if M is too small. Thus, we use $\sigma^2[i,j] = \max\left(0, \tilde{\sigma}^2[i,j]\right)$. With the estimated $\sigma[i,j]$ and σ_n, we apply a Wiener (least-squares fit) filter to all $\mathbf{Y}_m[i,j] \in \mathbf{Y}_m$, $m = 6, \ldots, 10$:

$$\widetilde{\mathbf{Y}}_m[i,j] = \frac{\sigma^2[i,j]}{\sigma^2[i,j] + \sigma^2_n}\mathbf{Y}_m[i,j]. \quad (5)$$

We can further decompose the output $\mathbf{Y}_0$ and denoise the wavelet outputs using the above described process. Our algorithm can be summarized as follows:

Algorithm 1 (UHDA1)

0: *Input the noisy image* $\mathbf{X}$*, a threshold factor* α*, and the number of decomposition levels* J.

1: *Decompose the image* $\mathbf{X}$ *up to level* J *using the UHF11 filter bank to obtain* $\mathbf{Y}_m$, $m = 0, \ldots, 10$.

2: *Compute* $\widetilde{\mathbf{Y}}_m$, $m = 1, \ldots, 10$. *using Equations* (2)–(5).

3: *Reconstruct image* $\widetilde{\mathbf{X}}$ *from* $\mathbf{Y}_0$ *and* $\widetilde{\mathbf{Y}}_m$, $m = 1, \ldots, 10$ *by using the UHF11 filter bank.*

We can improve UHDA1 as follows: Let w be a weight between 0 and 1. The linear combination $(1-w)\mathbf{X} + w\widetilde{\mathbf{X}}$ will be considered as a new noisy image. Using UHDA1, we obtain a new denoised image. We iterate the process and change the weight w:

Algorithm 2 (UHDA2)

0: *Set the weight vector* $w = [0.2, 0.4, 0.6, 0.8, 0.9]$. *Input the noisy image* $\mathbf{X}$*, a threshold factor* α*, and the number of decomposition levels* J.

1: *For* $k = 1, \ldots, length(w)$ *do*

Apply UHDA1 to $\mathbf{X}$ *to obtain* $\widetilde{\mathbf{X}}$

Replace $\mathbf{X}$ *by* $(1 - w(k))\mathbf{X} + w(k)\widetilde{\mathbf{X}}$

2: *Output* $\widetilde{\mathbf{X}}$*;*

Table 1. PSNR after iterative application of UHDA1 with various weights w.

w \ σ	10	15	20	25	30
Barbara ($\alpha = (1/4)$)					
0	32.59	29.90	27.96	26.50	25.38
0.2	32.72	30.10	28.17	26.71	25.57
0.4	32.83	30.27	28.40	26.94	25.79
0.6	32.89	30.42	28.60	27.18	26.04
0.8	32.88	30.46	28.74	27.36	26.24
0.9	32.73	30.56	28.80	27.45	26.36
Yogi ($\alpha = (\sqrt{2}/4)$)					
0	35.30	31.93	29.37	27.46	26.03
0.2	35.56	32.32	29.90	27.98	26.50
0.4	35.82	32.67	30.40	28.56	27.07
0.6	36.04	32.96	30.78	29.07	27.64
0.8	36.15	33.12	31.01	29.37	28.02
0.9	36.17	33.16	31.09	29.49	28.18

4. RESULTS

We tested our proposed algorithms on a number of images. In this section we present selected results for four. White Gaussian noise with zero-mean and standard deviation $\sigma_n = 10, 15, 20, 25, 30$ was added to the four images, and denoising performance was evaluated using peak signal-to-noise ratio (PSNR) in dB as a performance metric.

Performance results for the two proposed algorithms are presented in Table 1. The results with $w = 0$ are produced by UHDA1. We observe that the iterative application of UHDA1 with varying weights does improve the PSNR. It is reasonable to expect that this process cannot be used indefinitely, and will eventually lead to deteriorated performance. Thus, the choice of weights and the number of iterations necessary need to be carefully calibrated, with more iterations being admissible for larger noise levels. However, the particular choice of weights proposed in UHDA2 is shown to be quite adequate in finding a good balance, with gains over UHDA1 of up to 2 dB in some cases (such as the Yogi image).

We also benchmarked UHDA2 against various other methods reported in the literature. Here, we present results comparing it to three other methods (see Table 2). The first is implemented by the *wiener2* function in the software package MATLAB. We also tested implementations of the *bishrink* [13], and the GSM [10] algorithms. We observe that our method outperforms the others in terms of PSNR when applied to the Peppers and Yogi images, and produces similar results for the Boat image. Figure 1 depicts the results for the Peppers image. Note that our method produces denoised images that exhibit noticeably less ringing artifacts around edges compared to the other methods.

5. CONCLUSIONS

This paper developed a general theory of constructing new frames from existing ones. Starting from a piecewise linear spline tight frame in 1D, we designa Parseval frame lifted using our theory. These non-separable framelets are capable of detecting first order singularities in directions that are integer multiples of 45^o. To illustrate the appeal of these framelets, two image denoising algorithms were proposed, tailored to their specific properties. Our results indicate that our algorithms produce denoised images with less ringing artifacts and similar, or better, PSNR when compared to other state of the art algorithms.

ACKNOWLEDGEMENTS We would like to thank Javier Portilla and Eero Simoncelli for providing us with an early version of

Table 2. Comparison of PSNR values of results for different test images and noise levels σ; (a) *wiener2*, (b) *bishrink*, (c) GSM, and (d) UHDA2.

σ / PSNR	*wiener2*	*bishrink*	GSM	UHDA2
Peppers256 ($\alpha = (1/4)$)				
10 / 28.13	30.70	33.48	33.77	34.24
15 / 24.61	29.56	31.35	31.74	32.10
20 / 22.11	28.44	29.80	30.31	30.38
25 / 20.17	27.42	28.66	29.21	29.21
30 / 18.59	26.50	27.77	28.30	28.11
Yogi ($\alpha = (\sqrt{2}/4)$)				
10 / 28.13	30.67	33.99	33.92	36.17
15 / 24.61	29.26	31.13	31.26	33.16
20 / 22.11	27.91	29.19	29.45	31.09
25 / 20.17	26.71	27.78	28.11	29.49
30 / 18.59	25.68	26.70	27.05	28.18
Boat ($\alpha = (1/4)$)				
10 / 28.13	30.02	32.99	33.58	33.20
15 / 24.61	29.03	31.23	31.70	31.61
20 / 22.11	28.07	29.94	30.38	30.28
25 / 20.17	27.18	28.93	29.37	29.17
30 / 18.59	26.36	28.12	28.51	28.14

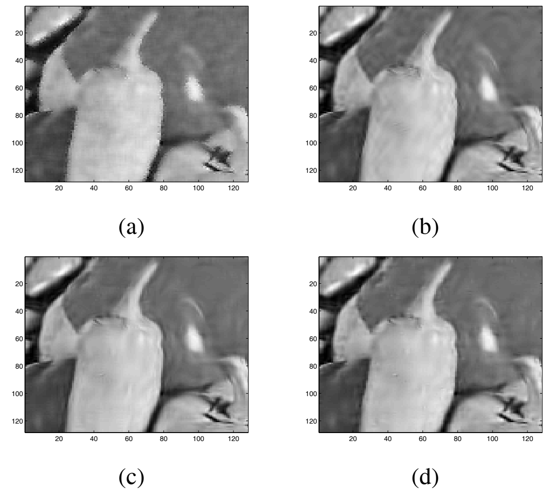

Fig. 1. Results of denoising the "Peppers" image with $\sigma = 20$, using (a) *wiener2*, (b) *bishrink*, (c) GSM, and (d) UHDA2.

their code in order to compare our results, and for their very helpful comments. This work was supported in part by NIH 5ROIEB00148-02, NSF IIS-9985482, NSF CHE-0074311 and Welch grant E-0608.

6. REFERENCES

[1] D. Donoho and I. Johnstone, "Ideal spatial adaptation via wavelet shrinkage," *Biometrika*, vol. 81, pp. 422–455, 1994.

[2] D. Donoho, "De–noising by Soft–Threshold," *IEEE Trans. on Information Theory*, vol. 41, pp. 613–627, 1995.

[3] D. Donoho and I. Johnstone, "Adapting to unknown smoothness via wavelet shrinkage," *J. of the Amer. Stat. Assoc.*, vol. 90, no. 432, pp. 1200–1224, 1995.

[4] R.R. Coifman and D.L. Donoho, "Translation-invariant denoising," in *Wavelets and Statistics*, Lecture Notes in Statistics, vol. 103, pp. 125–150. Springer-Verlag, Berlin, 1995.

[5] E. P. Simoncelli, "Bayesian denoising of visual images in the wavelet domain," in *Bayesian Inference in Wavelet Based Models*, Lecture Notes in Statistics, vol. 141, pp. 291–308. Springer-Verlag, New York, 1999.

[6] S.G. Chang, B. Yu, and M. Vetterli, "Spatially adaptive wavelet thresholding with context modeling for image denoising," *IEEE TIP*, vol. 9, no. 9, pp. 1522–1531, September 2000.

[7] X. Li and M. Orchard, "Spatially adaptive denoising under overcomplete expansion," in *Int'l Conf. on Image Proc.*, 2000, vol. 3, pp. 300–303, IEEE Sig Proc Society.

[8] H. Zhang, A. Nosratinia and R.O. Wells", "Modeling the autocorrelation of wavelet coefficients for image denoising," in *Int'l Conf. on Image Proc.*, 2000, vol. 3, pp. 304–307, IEEE Sig Proc Society.

[9] E. Simoncelli, W.T. Freeman, E. Adelson, and D. Heeger, "Shiftable multi-scale transforms," *IEEE Tran. on Information Theory*, vol. 38, no. 2, pp. 587–607, March 1992.

[10] J. Portilla, V. Strela, M. Wainwright, and E.P. Simoncelli, "Image denoising using scale mixtures of Gaussians in the wavelet domain," *IEEE TIP*, vol. 12, no. 11, pp. 1338–1351, November 2003.

[11] N.G. Kingsbury, "Complex wavelets for shift invariant analysis and filtering of signals," *Applied and Computational Harmonic Analysis*, pp. 234–253, May 2001.

[12] L. Sendur and I.W. Selesnick, "Bivariate shrinkage functions for wavelet-based denoising exploiting interscale dependency," *IEEE TSP*, vol. 50, no. 11, pp. 2744–2756, November 2002.

[13] L. Sendur and I.W. Selesnick, "Bivariate shrinkage with local variance estimation," *IEEE Signal Processing Letters*, vol. 9, no. 12, pp. 438–441, December 2002.

[14] E. P. Simoncelli and E. H. Adelson, "Noise removal via Bayesian wavelet coring," in *Third Int'l Conf. on Image Proc.*, 1996, vol. I, pp. 379–382, IEEE Sig Proc Society.

[15] M.K. Mihcak, I. Kozintsev, and K. Ramchandran, "Low-complexity image modeling based on statistical modeling of wavelet coefficients," *IEEE Signal Processing Letters*, vol. 6, no. 2, pp. 300–303, December 1999.

[16] J.M. Shapiro, "Embedded image coding using zerotrees of wavelet coefficients," *IEEE Tran. on Acoustics, Speech and Signal Processing*, vol. 41, no. 12, pp. 3445–3462, 1993.

[17] S. Mallat, *A Wavelet Tour of Signal Processing*, 2nd ed., Academic Press, 1999.

[18] M. Papadakis, G. Gogoshin, I.A. Kakadiaris, D.J. Kouri, and D.K. Hoffman, "Non-separable radial frame multiresolution analysis in multidimensions," *Numerical Functional Analysis and Optimization*, vol. 24, pp. 907–928, 2003.

[19] M. Papadakis, "Generalized frame multiresolution analysis in abstract Hilbert spaces," in *Sampling, Wavelets and Tomography*, J. J. Benedetto and A. Zayed, Eds. Birkhaüser, Boston, 2003.

[20] A. Ron and Z. Shen, "Affine system in $L^2(\mathbf{R}^d)$: the analysis of the analysis operator," *J. of Functional Analysis*, vol. 148, pp. 408–447, 1997.

[21] J.J. Benedetto and O. Treiber, "Wavelet frames: Multiresolution analysis and extension principles," in *Wavelet Transforms and Time–Frequency Analysis*, L. Debnath, Eds. Birkhaüser, Boston, 2001.